Analysis of the interface in a nonequilibrium two-temperature Ising model

P. I. Hurtado
Department of Physics, Boston University, Boston, Massachusetts 02215, USA
and Institute Carlos I for Theoretical and Computational Physics, Universidad de Granada, E-18071-Granada, Spain

P. L. Garrido and J. Marro
Institute Carlos I for Theoretical and Computational Physics, and Departamento de Electromagnetismo y Física de la Materia, Universidad de Granada, E-18071-Granada, Spain

(Received 22 May 2004; revised manuscript received 20 September 2004; published 6 December 2004)

The influence of nonequilibrium bulk conditions on the properties of the interfaces exhibited by a kinetic Ising-like model system with nonequilibrium steady states is studied. The system is maintained out of equilibrium by perturbing the familiar spin-flip dynamics at temperature T with completely random flips; one may interpret these as ideally simulating some (dynamic) impurities. We find evidence that, in the present case, the nonequilibrium mechanism adds to the basic thermal one resulting on a renormalization of microscopic parameters such as the probability of interfacial broken bonds. On this assumption, we develop theory for the nonequilibrium "surface tension," which happens to show a nonmonotonous behavior with a maximum at some finite T. The phase diagram, as derived from this effective interfacial free energy, exhibits reentrant behavior. In addition, interface fluctuations differ qualitatively from the equilibrium case, e.g., the interface remains rough at zero T, in full agreement with Monte Carlo simulations. We discuss on some consequences of these facts for nucleation theory, and make some explicit predictions concerning the nonequilibrium droplet structure.

DOI: 10.1103/PhysRevB.70.245409 PACS number(s): 68.35.-p, 05.70.Np

I. INTRODUCTION

Interfaces that separate different homogeneous media are familiar from many natural phenomena such as phase segregation, wetting processes, fluid dynamics, crystal growth, and molecular beam epitaxy, for instance. In practice, the interface may determine the system morphology and its critical properties, or the details of time evolution, which has motivated many specific studies during the last two decades.[1–7] The phenomena most deeply studied so far concern interfaces that separate *equilibrium* phases. However, the actual systems of interest are seldom at equilibrium and one often needs to be concerned with *nonequilibrium interfaces*, i.e., interfaces that separate nonequilibrium phases.[8–11] This paper aims towards a better understanding of how nonequilibrium conditions influence the properties of an interface. The results here will be applied in a forthcoming paper to analyze the exit from a (nonequilibrium) metastable state, which is an interface-controlled process.[12]

Mathematical complexity often compels one to deal with the simplest model situations. In this paper, we study interfaces in a two-dimensional kinetic Ising model. The nonequilibrium condition is obtained by perturbing the underlying stochastic dynamics in such a way that, in general, a nonequilibrium steady state is reached asymptotically (instead of the more familiar thermodynamic equilibrium state).[10] We develop for this case a simple approximation which predicts both microscopic and macroscopic properties for the (nonequilibrium) interface, namely, the profile or single-step height probability distribution and a (nonequilibrium) "surface tension" $\sigma_{\rm NE}$. The latter turns out to qualitatively differ from the equilibrium surface tension σ_e. In particular, $\sigma_{\rm NE}$ behaves nonmonotonously with decreasing temperature, and exhibits a maximum at some finite temperature, unlike σ_e that monotonously grows as one cools the system. In addition, the phase diagram of the model, as derived from this effective surface tension, exhibits reentrant behavior. We also predict that, due to the nonequilibrium perturbation, the interface in this model remains rough at zero temperature. In order to understand this behavior, we analyze the shape of a droplet of the minority phase, and conclude how the nonequilibrium condition substantially influences the low-temperature droplet morphology. Our predictions are compared with the results from computer simulations, which seem to firmly support them in general.

The paper is organized as follows. The model is defined in Sec. II, and Sec. III describes our approximation. The main results are in Sec. IV which also contains some details of the computer simulations and a comparison of the numerical results with theory. Section V is devoted to conclusions.

II. THE MODEL

Let the square lattice $\Lambda(L_x,L_y)\in\mathbb{Z}^2$ of size $N=L_x\times L_y$ with a binary spin variable $s_i=\pm 1$ at each node $i\in[1,N]$. We remind the reader that the two states of s_i may be interpreted as corresponding to the presence or absence, respectively, of a particle at i; this happens to provide a more intuitive picture concerning the phenomena of interest here. There is interaction between nearest-neighbor *spins* given by the Ising Hamiltonian

$$\mathcal{H} = -\sum_{\langle i,j \rangle} s_i s_j \tag{1}$$

and stochastic dynamics by single-spin flips. The latter occur with transition rate (per unit time) given by

$$\omega(s_i \to -s_i) = p + (1-p)\Psi(\beta \Delta \mathcal{H}_i). \tag{2}$$

Here, $\beta = 1/T$—we take both the coupling constant and the Boltzmann constant equal to unity—and $\Delta \mathcal{H}_i = 4 s_i (n_i - 2)$, where $n_i \in [0,4]$ is the number of up nearest-neighbor spins surrounding s_i, i.e., $\Delta \mathcal{H}_i$ measures the energy cost of flipping at i. The undetermined function in Eq. (2) is either $\Psi(\Gamma) = e^{-\Gamma}(1+e^{-\Gamma})^{-1}$ or $\Psi(\Gamma) = \min[1, e^{-\Gamma}]$; as indicated below, we are mostly concerned here with the first choice, except when the second one allows for an explicit or a simpler description. In any case, both choices lead to the results in this paper.

One may interpret that the parameter p in Eq. (2) balances the competition between two thermal baths: one is at temperature T, while the other induces completely random transitions as if it was at infinite temperature. For $p=0$, $\omega(s_i \to -s_i)$ satisfies detailed balance, and the system goes asymptotically to the equilibrium state for temperature T and energy $\mathcal{H}$. The system exhibits in this case the familiar, Onsager critical point at $T = T_C(p=0) = T_O = 2/\ln(1+\sqrt{2})$. Otherwise, $0 < p < 1$, the competition in Eq. (2) impedes canonical equilibrium and, in general, a nonequilibrium steady state sets in asymptotically with time. A critical point is still observed in this case, but at $T = T_C(p) < T_O$, as far as $p < p_c$. For $p > p_c$ the system remains in the disordered phase at any T. As shown below, our theoretical approach in this paper predicts $p_c = (\sqrt{2}-1)^2 \approx 0.1716$, in perfect agreement with previous Monte Carlo estimations.[10] In addition, when subject to an external magnetic field, this model exhibits metastable states whose strength decreases with increasing field, eventually becoming unstable. The spinodal field characterizing the limit of metastability undergoes an interesting reentrant phenomenon as a consequence of the nonlinear interplay between T and p.[13] We will show below that a similar reentrant behavior is observed for the phase diagram $T_C(p)$.

In the ordered phase below $T_C(p)$, this system exhibits an interface for appropriate boundary conditions. Consider, for instance, periodic boundary conditions along the $\hat{x}$ direction, and open boundaries along the $\hat{y}$ direction. Then let the spins in the bottom (top) row freeze in the up (down) state, while the rest of spins are allowed to change stochastically according to Eq. (2). Under these conditions, an interface eventually develops along the $\hat{x}$ direction that separates up- from down-spin rich regions located at the bottom and top of the system, respectively. For $p=0$ (the equilibrium case), the macroscopic properties of this interface are well known. In particular, its scaling behavior is characteristic of the Kardar-Parisi-Zhang universality class,[14] and one knows the total free energy per unit length or surface tension.[15] The question is how these properties are affected by the nonequilibrium perturbation parametrized by p.

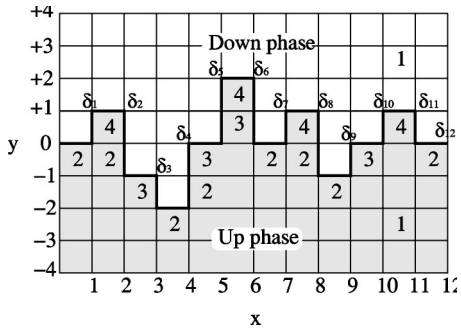

FIG. 1. Example of interface for $L_x = 12$ with steps $\delta = (1,-2,-1,2,2,-2,1,-2,1,1,-1,0)$. The numbers shown in the squares indicate the class of the corresponding spin as defined in the main text. Notice that interfacial spins can only belong to classes 2, 3, and 4.

III. SOLID-ON-SOLID APPROXIMATION

The interface is first analyzed here by adapting to our case the solid-on-solid (SOS) picture introduced by Burton, Cabrera, and Frank.[16] This assumes that the interface can be described by a single-valued discrete function completely defined by the set of interface steps $\{\delta_x, x \in [1, L_x]\}$, as illustrated in Fig. 1. No overhangs are allowed in this approximation. Furthermore, the heights of the individual steps are assumed to be independent. The probability of a step of height δ is assumed to be given by

$$P(\delta) = \frac{1}{z[T,p,\gamma(\phi)]} X(T,p)^{|\delta|} e^{\gamma(\phi)\delta}. \tag{3}$$

Here $X(T,p)$ is the statistical weight associated to a broken bond in the interface, and $\gamma(\phi)$ is a Lagrange multiplier intended to keep the average step value at a x-independent value $\langle \delta_x \rangle = \tan\phi$, where ϕ is the *average* angle between the interface and the $\hat{x}$ axis.[17,18] The function $z[T,p,\gamma]$ may be obtained from the normalization of Eq. (3), and the "partition function" for the SOS interface follows as $Z(T,p,\gamma) = [Xz(T,p,\gamma)]^{L_x}$. This allows one to define a "thermodynamic" potential $\varphi(T,p,\gamma) \equiv \lim_{L_x \to \infty} -(\beta L_x)^{-1} \ln Z$. Our interest is then on the "free energy" $\sigma'(T,p,\phi)$—defined as conjugated to the potential $\varphi(T,p,\gamma)$ via a Legendre transform, which involves the variables $\tan\phi$ and $T\gamma$—and, in particular, on its projection σ along the $\hat{x}$ axis. The nature of the above approximation is discussed below; we now remark that our use of equilibrium words here is only for simplicity and comfort. The general result is

$$\sigma(\phi) = T|\cos\phi| \left\{ \gamma(\phi)\tan\phi - \ln \frac{X(1-X^2)}{1 + X^2 - 2X\cosh\gamma(\phi)} \right\}. \tag{4}$$

In the equilibrium limit $p=0$, one has the weight $X(T,p=0) = e^{-2\beta}$, and $\sigma_e \equiv \sigma(T,p=0,\phi)$ is the SOS surface tension associated to the equilibrium Ising interface.[16–18] We shall assume in this paper that all the main effects of the nonequilibrium perturbation (p) on the interface can be taken into account after a proper generalization of the microscopic pa-

rameter $X(T,p)$. The function $\sigma_{\rm NE}\equiv\sigma(T,p>0,\phi)$ which results after using this generalization in Eq. (4) is therefore assumed to be the nonequilibrium "surface tension" in SOS approximation, and this is expected to capture the macroscopic properties of the nonequilibrium interface. The resulting $\sigma_{\rm NE}$ is to be interpreted as an *effective* free energy per unit length in the present case that lacks of a proper bulk free-energy function. This definition of nonequilibrium "surface tension" is based on the assumption that the normalization $Z(T,p,\gamma)$ of the probability measure associated to interface configurations in SOS picture is some sort of nonequilibrium analog of the partition function. Similar hypotheses have been shown to yield excellent results when applied to other nonequilibrium models.[19] For instance, in the one-dimensional asymmetric simple exclusion process (ASEP) with open boundaries, the distribution of (complex) zeros of the steady-state normalization factor has been shown to obey the Lee-Yang picture of phase transitions.[19]

In the simplest scenario—which is consistent with the equilibrium limit—the weight $X(T,p)$ will not depend on $\gamma(\phi)$. An explicit relation between $\gamma(\phi)$ and $\tan\phi$ can then be obtained. In particular, using $\langle\delta_x\rangle=\tan\phi$, one finds that

$$e^{\pm\gamma(\phi)}=\frac{(1+X^2)\tan\phi\pm S(\phi)}{2X(\tan\phi\pm 1)}, \tag{5}$$

$$z(\phi)=\frac{(1-X^2)(1-\tan^2\phi)}{1+X^2-S(\phi)}, \tag{6}$$

where $S(\phi)=[(1-X^2)^2\tan^2\phi+4X^2]^{1/2}$ and we dropped an obvious dependence on T and p. The nonequilibrium surface tension (4) may now be explicitly written as

$$\sigma(\phi)=T|\cos\phi|\left\{(\tan\phi)\ln\frac{(1+X^2)\tan\phi+S(\phi)}{2X(\tan\phi+1)}-\ln\frac{X(1-X^2)(1-\tan^2\phi)}{1+X^2-S(\phi)}\right\}. \tag{7}$$

Equations (3) and (7) are two important properties of the interface at the microscopic and macroscopic levels of description, respectively. Interesting enough, Eq. (7) reduces in equilibrium ($p=0$) to the known *exact* result for $\phi=0$. It also yields a very good approximation for any angle $|\phi|<\pi/4$;[15,20] for $|\phi|>\pi/4$, it is convenient to turn to the $\hat{y}$ (instead of $\hat{x}$) axis as the reference frame. $\sigma(T,p=0,\phi=0)$ is a monotonously decreasing function of T, which converges toward 2 as $T\to 0$, and vanishes at the exact Onsager critical temperature. In addition, the angular dependence of $\sigma(T,p=0,\phi)$ may be used to determine the equilibrium crystal shape via minimization of the total surface tension for a fixed volume in a homogeneous droplet (Wulff construction).

A. Statistical weight of a broken bond

At equilibrium, the weight equals the Boltzmann factor $X(T,p=0)=e^{-2\beta}$ (2 is the energy cost of a broken bond). More generally, $0<p<1$, the weight of a broken bond depends on the local order surrounding the spin at the end of the bond. One may say that $X(T,p)$ depends on the *class* of this spin. The spin s_i is said to be of class $\eta(s_i,n_i)=3-s_i(n_i-2)$, where n_i is the number of up nearest-neighbor spins of s_i. That is, our model may exhibit up to five different classes of spins $\eta=1,\ldots,5$.[21] All the spins in a given class are characterized by the same value of $\Delta\mathcal{H}_\eta=4s_i(n_i-2)$ and, consequently, by the same rate, Eq. (2).

The function $X_\eta(T,p)$ for class η now follows straightforwardly. Consider Eq. (2) with $\Psi(\Gamma)=\min[1,e^{-\Gamma}]$ which allows for a simpler and more explicit discussion.[22] If, for instance, a spin in class $\eta=1$ is flipped, four new broken bonds appear. Since $\Delta\mathcal{H}_1=8$, one immediately has that $X_1(T,p)=[p+(1-p)e^{-8\beta}]^{1/4}$ for the first class. Equivalently, $X_2(T,p)=[p+(1-p)e^{-4\beta}]^{1/2}$ for the second class, and the rest are characterized by the same weight as in equilibrium $X_3(T,p)=X_4(T,p)=X_5(T,p)=X(T,p=0)$. It follows that $X_1<X_2<X_{3,4,5}$ for any $0<p<1$, and one may also see that $X_\eta(T,p\to 0)\to e^{-2\beta}$, independent of η as expected.

As illustrated in Fig. 1, interfacial spins may only belong to classes 2, 3, and 4; class 1 corresponds to spins in the bulk of (either up or down) homogeneous regions and class 5 corresponds to typical isolated fluctuations in the bulk. Consequently, for the case in consideration,[22] only two weights X_2 and $X_3=X_4$ are relevant. An even simpler description ensues assuming, which amounts a reasonable mean-field approximation, that interfacial broken bonds have an unique statistical weight equal to the *weighted* average of X_2 and X_3, namely,

$$X(T,p)=\Pi_2(T,p)X_2(T,p)+[\Pi_3(T,p)+\Pi_4(T,p)]X_3(T,p). \tag{8}$$

Here, $\Pi_\eta(T,p)$ is the probability of an interfacial broken bond associated to a spin of class η. Alternatively, given that any bond can be arbitrarily associated to any of the two spins at the ends, we may interpret $\Pi_\eta(T,p)$ as the probability of an interfacial *up* spin of class η. Therefore, $\Pi_2(T,p)+\Pi_3(T,p)+\Pi_4(T,p)=1$.

B. Population of interfacial spin classes

Next, we estimate the population densities $\Pi_\eta(T,p)$, which requires a detailed counting beyond the SOS approximation. Let $P(\delta,\epsilon)$ the joint probability that a step variable equals δ and the step variable at its right is ϵ. This completely characterizes the population of each interfacial class in the involved column. Consider, for instance, the case $\delta,\epsilon>0$, as in the column between $x=4$ and $x=5$ in Fig. 1. This column contains $\delta+\epsilon$ interfacial spins, of which $\delta+\epsilon-2$ are of class 2 and the other two spins are of class 3. On the other hand, this configuration involves $\delta+\epsilon+1$ broken bonds, of which $\delta+1$ belong to up spins in this column; following our convention above, the other ϵ broken bonds may be associated with the up interfacial spins in the column between $x+1$ and $x+2$. In order to go further in the analytical solution of the problem, let us neglect column-column correlations by assuming that broken bonds in the interfacial column are to be associated to interfacial spins in this column. For $\delta,\epsilon>0$, one has $\delta+\epsilon-2$ broken bonds associated to interfacial spins of class 2, and three broken bonds associated to spins

TABLE I. The nine different typical configurations of an interfacial spin column in our approximation. These configurations are defined by the signs of the left, δ and right ϵ steps. The last column shows the probability $P(\delta,\epsilon)$ of each configuration. Here, $\alpha \equiv \min(|\delta|,|\epsilon|)$ and $\lambda \equiv \max(|\delta|,|\epsilon|)$; see the main text for other definitions.

Step variables	Configuration	$P(\delta,\epsilon)\times\mathcal{Q}$
$\delta>0,\ \epsilon>0$	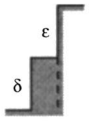	$\Lambda^{\delta+\epsilon}X_2^{\delta+\epsilon-2}X_3^3$
$\delta>0,\ \epsilon=0$		$\Lambda^{\delta}X_2^{\delta-1}X_3^2$
$\delta>0,\ \epsilon<0$		$\Lambda^{\delta+\epsilon}X_2^{\lambda-\alpha}X_3^{2\alpha+1}$
$\delta=0,\ \epsilon>0$		$\Lambda^{\epsilon}X_2^{\epsilon-1}X_3^2$
$\delta=0,\ \epsilon=0$		X_2
$\delta=0,\ \epsilon<0$		$\Lambda^{\epsilon}X_2^{\lvert\epsilon\rvert-1}X_3^2$
$\delta<0,\ \epsilon>0$	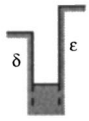	$\Lambda^{\delta+\epsilon}X_9^{\lambda-\alpha}X_3^{2\alpha+1}$
$\delta<0,\ \epsilon=0$		$\Lambda^{\delta}X_2^{\lvert\delta\rvert-1}X_3^2$
$\delta<0,\ \epsilon<0$	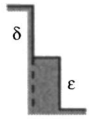	$\Lambda^{\delta+\epsilon}X_2^{\lvert\delta\rvert+\lvert\epsilon\rvert-2}X_3^3$

of class 3. Let us assume also that, in general, the probability of a given interfacial column configuration is proportional to the product of probabilities of each of the broken bonds which form it. We have that

$$P(\delta>0,\epsilon>0)=\frac{1}{\mathcal{Q}}\{\Lambda^{\delta+\epsilon}X_2^{\delta+\epsilon-2}X_3^3\},$$

where $\mathcal{Q}$ is a normalization factor and $\Lambda(\phi)\equiv e^{\gamma(\phi)}$.[23] Equivalently, for $\delta>0$ and $\epsilon<0$ one may write that

$$P(\delta>0,\epsilon<0)=\frac{1}{\mathcal{Q}}\{\Lambda^{\delta+\epsilon}X_2^{\lambda-\alpha}X_3^{2\alpha+1}\},$$

where $\alpha=\min(|\delta|,|\epsilon|)$ and $\lambda=\max(|\delta|,|\epsilon|)$. Table I shows all of the possible interfacial column configurations, together with their statistical weights. Notice that, as one may conclude from Table I and Eq. (3), the probabilities $P(\delta,\epsilon)$ converge as $p\to 0$ to the SOS equilibrium value $XP(\delta)P(\epsilon)$.

TABLE II. Number $n_\eta(\delta,\epsilon)$ of up interfacial spins of class $\eta=2,3,4$ for the column configuration types defined in Table I. The last column shows the total number of up interfacial spins associated to each type.

Step variables	$n_2(\delta,\epsilon)$	$n_3(\delta,\epsilon)$	$n_4(\delta,\epsilon)$	$N(\delta,\epsilon)$
$\delta>0,\ \epsilon>0$	$\delta-1$	1	0	δ
$\delta>0,\ \epsilon=0$	$\delta-1$	1	0	δ
$\delta>0,\ \epsilon<0$	$\lambda-\alpha$	$\alpha-1$	1	λ
$\delta=0,\ \epsilon>0$	1	0	0	1
$\delta=0,\ \epsilon=0$	1	0	0	1
$\delta=0,\ \epsilon<0$	$\lvert\epsilon\rvert-1$	1	0	$\lvert\epsilon\rvert$
$\delta<0,\ \epsilon>0$	1	0	0	1
$\delta<0,\ \epsilon=0$	1	0	0	1
$\delta<0,\ \epsilon<0$	$\lvert\epsilon\rvert-1$	1	0	$\lvert\epsilon\rvert$

The densities $\Pi_\eta(T,p)$ may be written as an average over all possible interfacial column configurations

$$\Pi_\eta(T,p)=\sum_{\delta,\epsilon=-\infty}^{\infty}\pi_\eta(\delta,\epsilon)P(\delta,\epsilon). \tag{9}$$

Here, $\pi_\eta(\delta,\epsilon)$ is the probability of finding an *up* spin of class $\eta\in[2,4]$ in an interfacial column characterized by the pair (δ,ϵ). In general, $\pi_\eta(\delta,\epsilon)=n_\eta(\delta,\epsilon)/N(\delta,\epsilon)$, where $n_\eta(\delta,\epsilon)$ is the number of *up* spins of class η in an interfacial column characterized by (δ,ϵ), and $N(\delta,\epsilon)$ is the total number of *up* interfacial spins associated to this column. Table II shows $n_i(\delta,\epsilon)$ and $N(\delta,\epsilon)$ for all possible configurations.

The densities (9) will depend on the average interface slope $\tan\phi$ through the Lagrangian multiplier $\gamma(\phi)$. This dependence is inherited in general by the average weight of a broken bond in the nonequilibrium regime $X(T,p)$, see Eq. (8), and it makes the explicit calculation of the nonequilibrium surface tension unfeasible, see Sec. III A. Therefore, further simplifications are needed. We shall assume that the densities $\Pi_\eta(T,p)$ in Eq. (9) correspond to the case $\tan\phi=0$, i.e., $\Lambda(\phi)\equiv e^{\gamma(\phi)}=1$. In fact, the underlying lattice anisotropy implies that the interface tends in general to orientate parallel to any of the principal axis, which has a lower energy cost. Therefore, for regions of the parameter space (T,p) where such tendency is strong, it is justified to particularize the populations $\Pi_\eta(T,p)$ to the case $\tan\phi=0$. On the other hand, the parameter-space regions in which that tendency is weak are characterized by an effective isotropy, so that particularizing to a given orientation, e.g., $\tan\phi=0$ is valid. This approximation amounts to assume that the relevant orientation dependence entering the definition of the nonequilibrium surface tension (4) comes from the dependence on $\Lambda(\phi)$ that appears in the probability $P(\delta)$ of a step of size δ in the interface, see Eq. (3). A higher order, iterative procedure to take into account the ϕ dependence of $X(T,p$

>0) would consist in (i) calculate $X^{(0)} \equiv X(T,p)$ using the $\tan\phi=0$ simplification, (ii) use $X^{(0)}$ to compute $\Lambda^{(0)}(\phi)$ as a function of ϕ from Eq. (5), (iii) replace $\Lambda^{(0)}(\phi)$ in the general, $\Lambda(\phi)$-dependent expression for $X(T,p)$, and use the so-defined $X^{(1)}$ in Eq. (7) to compute an improved approximation to the nonequilibrium surface tension. We do not expect this complex procedure to produce a significative improvement of our approximation (while the resulting formulas are much more involved).

Assuming $\Lambda(\phi)=1$, and using $\pi_\eta(\delta,\epsilon)$ as given in Table II, we obtain from Eq. (9) that

$$\Pi_2 = \frac{X_3^2}{\mathcal{Q}}\left\{ \frac{2X_3}{(1-X_2)^2} + \frac{2}{1-X_2}\left[2+\frac{X_3}{X_2}\ln(1-X_3^2)\right] + \frac{2}{X_2}\ln(1-X_2) + \frac{X_2X_3}{1-X_2}\left[\frac{3}{X_2-X_3^2}+\frac{1}{1-X_3^2}\right] + \frac{X_3}{X_2-X_3^2}\left[\frac{2}{X_2-X_3^2}\ln\frac{1-X_2}{1-X_3^2} - \frac{X_3^2}{1-X_3^2}\right] + \frac{X_2}{X_3^2}\right\}. \tag{10}$$

The same method leads to

$$\Pi_4 = \frac{X_3X_2}{\mathcal{Q}(X_2-X_3^2)}\left[\frac{X_3^2}{X_2}\ln\frac{1-X_3^2}{(1-X_2)^2} + \ln(1-X_3^2)\right], \tag{11}$$

and the normalization condition gives $\Pi_3(T,p)=1-\Pi_2(T,p)-\Pi_4(T,p)$. The factor $\mathcal{Q}$ follows from the normalization of $P(\delta,\epsilon)$ for $\Lambda(\phi)=1$ as

$$\mathcal{Q} = \frac{2X_3^2}{1-X_2}\left\{2+\frac{X_3}{1-X_2}+\frac{X_3X_2}{X_2-X_3^2} - \frac{(1-X_2)X_3^3}{(X_2-X_3^2)(1-X_3^2)} + \frac{X_3X_2}{1-X_3^2}\right\} + X_2.$$

In equilibrium $p=0$, where $X_\eta(T,p)\to X(T,p=0)=e^{-2\beta}$, the above expressions for $\Pi_\eta(T,p)$ reduce to the known SOS equilibrium results.[18]

IV. SOME RESULTS

We summarize in this section some main results that follow from the above for the properties of the nonequilibrium interface and compare our predictions with Monte Carlo simulation data.

A. Microscopic structure

The basic SOS hypothesis is that the probability of a step of size δ in the nonequilibrium interface is given by Eq. (3). That is, $P(\delta)$ is an exponentially decaying function of $|\delta|$ controlled by a typical scale which, for $\tan\phi=0$, is $\overline{\delta}=|\ln X(T,p)|^{-1}$ with X given in Eq. (8). In order to check this assumption on the microscopic structure of the interface, we performed Monte Carlo simulations of the system in Sec. II. This evolved with time in the computer starting with two stripes of the same width of up and down spins, respectively, separated by a flat interface. We suppressed bulk dynamics in these simulations, i.e., bulk, class-1 spins remained frozen to prevent the nucleation of droplets in the bulk to interfere the interface dynamics. This turns out to simplify notably the analysis while it does not modify essentially the interface structure except close to the critical temperature, where fluctuation of all sizes occur. In fact, we carefully checked the validity of this assertion by computer simulations.

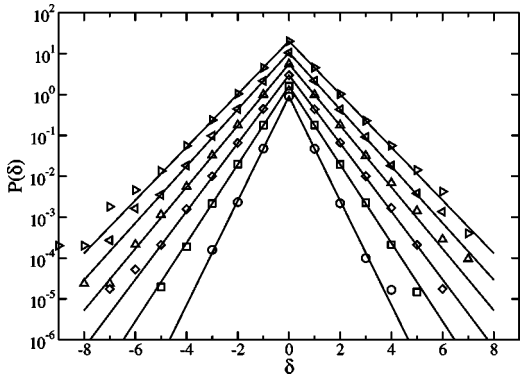

FIG. 2. The symbols are Monte Carlo results for the probability of step δ for a system of size $L_x\times L_y=256\times128$ at temperature $T=0.3T_O$, with $\tan\phi=0$ and different values of the nonequilibrium perturbation, namely, $p=0$, 0.01, 0.02, 0.03, 0.04, and 0.05 from bottom to top. Solid lines are the corresponding theoretical prediction (3). For the shake of clarity, the curves are shifted by a factor 2^i, $i\in[0,5]$ in the vertical direction, where $i=100\times p$.

The interface was thus observed to eventually reach a steady state, in which we measured the interface microscopic structure as a time average of $\delta=\{\delta_i, i=1,\ldots,L_x\}$—taking into account some (small) correlations observed between neighboring steps. Figure 2 depicts $P(\delta)$ as obtained for a (relatively large) system at low temperature for an average interface slope such that $\tan\phi=0$. The figure shows also our theoretical prediction (3), revealing an excellent agreement for all values of p. It is noticeable that the typical step scale $\overline{\delta}$ increases as p increases at fixed T, i.e., the nonequilibrium noise tends to amplify the interface fluctuations, as one should have probably expected.

Our data is good enough to provide an estimate for the second central moment of the step distribution, which measures the interface width $w^2(T,p)=\langle\delta^2\rangle-\tan^2\phi$. Our theoretical prediction is

$$w^2(T,p) = \frac{X\Lambda}{z(\phi)}\left[\frac{1}{(1-X\Lambda)^2}+\frac{1}{(\Lambda-X)^2} + \frac{2X\Lambda}{(1-X\Lambda)^3}+\frac{2X}{(\Lambda-X)^3}\right] - \tan^2\phi, \tag{12}$$

where $\Lambda(\phi)$, $z(\phi)$, and $X(T,p)$ are given by Eqs. (5), (6), and (8), respectively. Figure 3 compares this with Monte Carlo estimates. The most noticeable fact here is that $w^2(T,p)$ extrapolates towards a nonzero value in the low-temperature limit for any $p>0$, contrary to the case of an equilibrium interface, which is completely flat at zero temperature. That is, nonequilibrium fluctuations imply a rough interface even at zero temperature. The low-temperature roughness may be

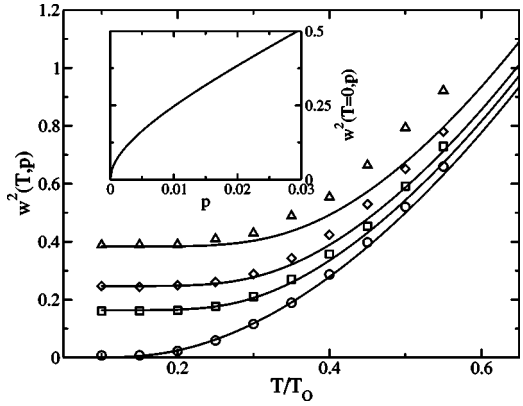

FIG. 3. The symbols are Monte Carlo results for the interfacial width $w^2(T,p)$ as a function of temperature for a system of size $L_x \times L_y = 256 \times 128$, tan $\phi = 0$, and, from bottom to top, $p = 0$, 0.005, 0.01, and 0.02. Errorbars are smaller that the symbol sizes. Solid lines are the corresponding theoretical prediction. Notice the nonzero interfacial width in the low-temperature limit for the nonequilibrium system ($p > 0$). The inset shows the SOS zero-temperature limit for the interfacial width $w^2(T=0,p)$, see Eq. (13), as a function of p.

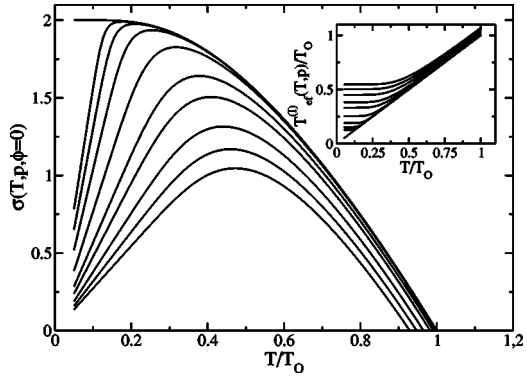

FIG. 4. Main graph: Theoretical prediction for the surface tension as a function of temperature for, from top to bottom, $p = 0$, 10^{-6}, 10^{-5}, 10^{-4}, 10^{-3}, 5×10^{-3}, 10^{-2}, 2×10^{-2}, 3×10^{-2}, and 4×10^{-2}. Notice that, for any—even small—$p > 0$, the surface tension behaves nonmonotonously, contrary to the equilibrium case. Inset: The effective interface temperature $T_{\rm ef}^{(I)}$, as defined in the main text, as a function of T for the same values of p than in the main graph. Notice that $T_{\rm ef}^{(I)}(T, p > 0)$ strongly deviates from T in the low-temperature regime.

estimated by realizing that, for $T \to 0$ and moderate values of p, $\Pi_2(T,p) \sim 1$ from Eq. (10), i.e., almost all interfacial up spins belong to class 2. Therefore, $X(T,p) \to X_2(T=0,p) = \sqrt{p}$ in this limit, so that one has for tan $\phi = 0$ that

$$w^2(T=0,p) \approx \frac{2\sqrt{p}}{(1-\sqrt{p})^2}. \tag{13}$$

The inset in Fig. 3 depicts this behavior which is in full agreement with our Monte Carlo values. The only significant differences we found between theory and simulations are at high enough temperatures, as illustrated in Fig. 3. This is to be attributed to step-step correlations as the critical temperature is approached.

B. Macroscopic behavior

A principal interface macroscopic property is the surface tension. The prediction (7) is illustrated in Fig. 4 for $\phi = 0$. It is remarkable the essential difference occurring at low T between the equilibrium and nonequilibrium cases.

The surface tension $\sigma_{\rm NE}(T, p > 0; \phi = 0)$ exhibits nonmonotonous behavior as a function of T, with a maximum at a temperature which depends on the intensity of the nonequilibrium perturbation $T_{\rm max}(p)$. For $T < T_{\rm max}(p)$, $\sigma_{\rm NE}$ decreases as one cools the system. This *anomalous* behavior turns out to play a fundamental role in understanding the exit from metastable states in this system,[11,12] and it is likely it may help the understanding of the low-temperature behavior in other complex systems concerning nucleation and growth processes.

We devised the following indirect method to check our predictions for the nonequilibrium surface tension. The system defined in Sec. II happens to exhibit long-lived metastable states in the ordered phase when subject to a small negative external magnetic field.[12,13] The exit from this state is a highly inhomogeneous process that proceeds via the nucleation and growth of one or several droplets of the stable phase within the metastable sea. Droplet nucleation is controlled by the competition between the surface tension, which hinders the droplet growth, and the bulk "free energy," which favors it. Consequently, small droplets—having a large surface/volume ratio—tend to shrink, while the larger ones tend to grow. The critical droplet size $R_c(T,p)$ separates these two regimes. Following further the trend in equilibrium theory,[12] one may assume that an effective macroscopic potential controls the escape from the metastable state for $0 < p < 1$, and that

$$R_c(T,p) = \frac{(d-1)\sigma(T,p)}{2m_s(T,p)|h}. \tag{14}$$

Here, d is the system dimensionality, h is the applied magnetic field, $\sigma(T,p)$ stands for the zero-field surface tension along one of the lattice axes, and $m_s(T,p)$ is the spontaneous (positive) magnetization for $h = 0$. The latter may be approximated by mean-field theory,[13] and the surface tension may then be obtained from a Monte Carlo estimate of $R_c(T,p)$.

In order to perform this computation, consider our system in a square lattice with periodic boundary conditions along both the $\hat{x}$ and $\hat{y}$ directions. The Hamiltonian is now $\mathcal{H}' = \mathcal{H} - h\Sigma_i s_i$, with $\mathcal{H}$ given in Eq. (1) and $h < 0$. All the spins are initially up, except for a *square* droplet of down spins of side $2R$ which represents the stable phase. This is let to evolve according to Eq. (2). The state is highly unstable, so that any *subcritical* initial cluster, i.e., $R < R_c(T,p)$, will very quickly shrink, while a *supercritical* one $R > R_c(T,p)$, will rapidly grow to cover the whole system. Since our dynamics is stochastic, we define the probability that a droplet of size R is supercritical $P_{\rm spc}(R)$. This is measured in practice by simply repeating many times the simulation and counting the number of times that the initial droplet grows to cover the

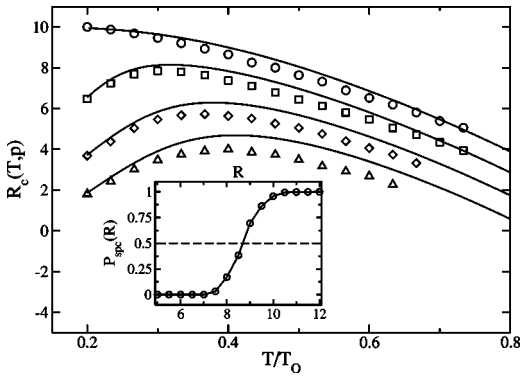

FIG. 5. Critical droplet size $\mathcal{R}_c$ as a function of temperature for a system of size $L=53$, with periodic boundary conditions, subject to a magnetic field $h=-0.1$ and, from top to bottom, $p=0$, 0.001, 0.005, and 0.01. The symbols are Monte Carlo results obtained as an average over $N_{\rm exp}=1000$ independent "experiments." The solid curves correspond to the theoretical prediction (14). For the sake of clarity, results for the nth value of p, $n=1,\ldots,4$ (using the above indicated order) have been shifted by $(1-n)$ units along the $\hat{y}$ axis. The inset shows Monte Carlo results for the probability that a droplet of radius R is supercritical $P_{\rm spc}(R)$ as a function of R for a system of size $L=53$ at $T=0.4T_O$, $p=0$, and $h=-0.1$. This corresponds to 10^3 independent experiments for each value of R. In all cases, error bars are smaller than the symbol sizes.

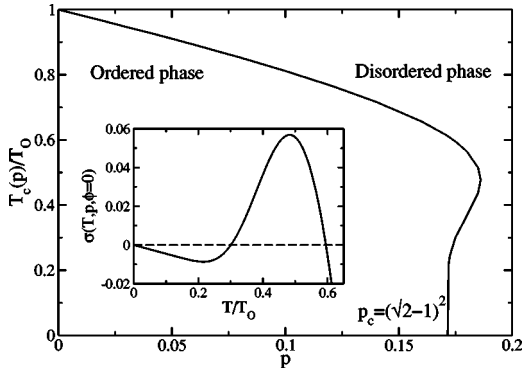

FIG. 6. Phase diagram of the model as obtained from the nonequilibrium surface tension. Notice the reentrant behavior of $T_C(p)$ for $p_c<p<p_c^*$, with $p_c=(\sqrt{2}-1)^2$ and $p_c^*\approx 0.18625$. Inset: $\sigma_{\rm NE}(\phi=0)$ as a function of T for $p=0.175>p_c$. Notice the negative slope at low-T and the intermediate temperature regime where $\sigma_{\rm NE}$ is positive.

system. The critical droplet size is defined by $P_{\rm spc}(R_c)=0.5$. As observed in the inset of Fig. 5, $P_{\rm spc}(R)$ sharply goes from 0 to 1, which allows a relatively accurate estimate of R_c.

Figure 5 compares our Monte Carlo results for $R_c(T,p)$ with the theoretical prediction from Eq. (14) using $\sigma(T,p)=\sigma_{\rm NE}(T,p;\phi=0)$ as given by Eq. (7). The agreement is rather good, and we confirm that $R_c(T,p)$ behaves nonmonotonously with T in the nonequilibrium regime.

The temperature dependence of $\sigma_{\rm NE}(T,p;\phi=0)$ may be used to compute the phase diagram of the model $T_C(p)$.[24] In equilibrium, the interface free energy approaches zero as $T\to T_O$; for $T>T_O$ there is no surface tension because there exist only one disordered phase.[24] Therefore, if as assumed in this paper $\sigma_{\rm NE}$ captures the macroscopic properties of the nonequilibrium interface, we may identify $T_C(p)$ as the temperature (other than $T=0$) for which $\sigma_{\rm NE}(T,p,\phi=0)=0$. This is done in Fig. 6. In particular, we may ask about the nonequilibrium parameter p_c above which no ordered phase exists at low T. For $p>0$ and $T\to 0$, $\sigma_{\rm NE}(T,p;\phi=0)\sim\alpha(p)T$ [see Fig. 4 and Eq. (7)]. The slope $\alpha(p)$ decreases monotonously with p, and the condition $\alpha(p_c)=0$ signals the onset of disorder at low temperature. This yields $p_c=(\sqrt{2}-1)^2\approx 0.1716$, in excellent agreement with previous Monte Carlo simulations.[10] For $p>p_c$ one does not expect low-T order. However, the nonmonotonous temperature dependence of $\sigma_{\rm NE}$ (see inset in Fig. 6) involves the emergence of an intermediate-T region for $p_c<p<p_c^*\approx 0.18625$ where order sets in, as opposed to the low-T and high-T disordered phases, see Fig. 6. This reentrant behavior of $T_C(p)$ is similar in spirit to the one reported in Ref. 13 for the spinodal field characterizing the limit of metastability in this model, and it is reminiscent of the reentrant phase diagram observed in systems subject to multiplicative noise.[25]

In order to gain some intuition on the physical origin of the anomalous low–temperature behavior of the nonequilibrium surface tension, let us write the statistical weight of an interfacial broken bond as

$$X(T,p)=\exp[-2\beta_{\rm ef}^{(I)}], \tag{15}$$

which defines an *interface effective temperature*. The function $T_{\rm ef}^{(I)}(T,p)=1/\beta_{\rm ef}^{(I)}$ is illustrated in the inset of Fig. 4. One first realizes that $T_{\rm ef}^{(I)}(T,p>0)>T$ for any $T\in[0,T_O]$. That is, the nonequilibrium interface endures an effective temperature larger than the thermodynamic one. On the other hand, one identifies two different regimes in the inset of Fig. 4 at given p. At high-T, where thermal fluctuations dominate over the nonequilibrium noise, $T_{\rm ef}^{(I)}$ is proportional to T. However, at low enough T the nonequilibrium noise dominates; in this case $T_{\rm ef}^{(I)}$ deviates from T and tends to a saturating, constant value which depends on p. Following the method above to obtain the zero-temperature interfacial width, we conclude that

$$\lim_{T\to 0} T_{\rm ef}^{(I)}(T,p)\approx -\frac{4}{\ln p}>0. \tag{16}$$

It is also remarkable that the onset of the deviation of $T_{\rm ef}^{(I)}$ from T for a given p coincides with the maximum observed for the nonequilibrium surface tension; see Fig. 4. In fact, since $T_{\rm ef}^{(I)}$ is a small constant for $0<T\ll T_C(p)$ and $p\ll p_c$, we may expand $\sigma_{\rm NE}$ at low-T to obtain $\sigma_{\rm NE}\sim(T/T_{\rm ef}^{(I)})\sigma_e+\mathcal{O}(TX)$. On the other hand, for $0\ll T<T_C(p)$ and the same $p\ll p_c$, the quotient $T/T_{\rm ef}^{(I)}\equiv 1-\alpha$ is a constant, with $0<\alpha\ll 1$. Using α as small parameter now, a high-T expansion of $\sigma_{\rm NE}$ yields $\sigma_{\rm NE}\sim(T/T_{\rm ef}^{(I)})\sigma_e+O(\alpha)$. In both limits the corrections to the asymptotic behavior $\sigma_{\rm NE}\sim(T/T_{\rm ef}^{(I)})\sigma_e$ are small. Now, since $T_{\rm ef}^{(I)}\sim$ constant and $\sigma_e\sim 2(1-Te^{-2/T})$ as $T\to 0$, one expects $\sigma_{\rm NE}$ to be an increasing function of T in this limit. On the other hand, $T/T_{\rm ef}^{(I)}\sim$ constant in the high-T limit, so $\sigma_{\rm NE}$ depends on T as σ_e does, i.e., $\sigma_{\rm NE}$ decreases with T for high enough T. Therefore one would expect a

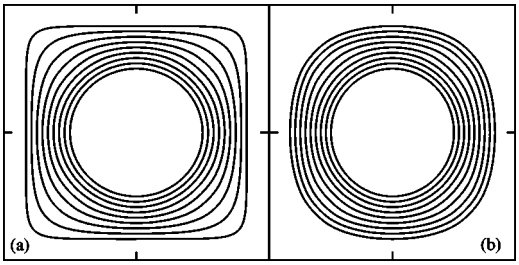

FIG. 7. (a) Shape of a droplet, as obtained from the Wulff construction, for $p=0$ (equilibrium) at, following to the center, $T/T_O = 0.1$, 0.2, 0.3, 0.4, 0.5, 0.6, 0.7, 0.8, and 0.9. For the sake of clarity we have rescaled the droplet according to its temperature. (b) The same as in (a), but for the nonequilibrium model with $p=0.01$.

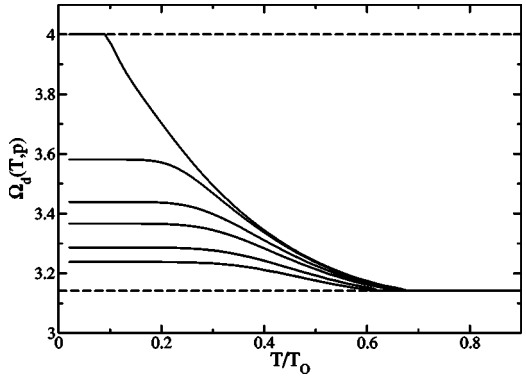

FIG. 8. The form factor $\Omega(T,p)$ as a function of temperature for, from top to bottom, $p=0$, 0.001, 0.005, 0.01, 0.02, and 0.03. The top (bottom) line corresponds to the squared (circular) droplet.

nonmonotonous T dependence of σ_{NE}, with a maximum at $T_{max}(p)$, which roughly coincides with the crossover observed in $T_{ef}^{(I)}(T,p)$. In this way, the anomalous T dependence of σ_{NE} can be traced back to the crossover between a T-dominated, high-T regime and a p-dominated, low-T region, as captured by $T_{ef}^{(I)}$.

C. Droplet shape

The droplet shape is controlled by the need to minimize the total surface tension at constant droplet volume. For isotropic systems, this implies spherical shape. In our case, however, the surface tension depends on the orientation of the interface with respect to a privileged axis $\sigma(\phi)$. Consequently, the shape adjusts itself to take advantage of the low free energy cost of certain interface orientations, which produces droplets with a crystal-like appearance which depends on temperature and other parameters.[26] We apply next the Wulff construction[27] to obtain information concerning the nonequilibrium droplet shape.

The method essentially consists in considering the polar curve $\sigma(\phi)$, $\phi \in [0, 2\pi]$, and drawing through its points a line perpendicular to the radius. The interior envelope to these lines determines the droplet radial function in polar coordinates $R(\theta)$. More specifically, one may write parametrically[28]

$$R(\theta) = R_0[x^2(\phi) + y^2(\phi)]^{1/2},$$

$$x(\phi) = \sigma(\phi)\cos\phi - \frac{d\sigma(\phi)}{d\phi}\sin\phi,$$

$$y(\phi) = \sigma(\phi)\sin\phi - \frac{d\sigma(\phi)}{d\phi}\cos\phi,$$

$$\tan\theta = \frac{y(\phi)}{x(\phi)}, \tag{17}$$

where R_0 is a fixed length scale and $\sigma(\phi)$ is the surface tension. We approximate the latter by Eq. (7). This is needed only for the angular interval $\phi \in [0, \pi/4]$, since one may extend then to the whole circumference by straightforward symmetry considerations. The result is singular for angles $\phi = (2n+1)\pi/4$, $n=0,\ldots,3$, which gives rise to angular intervals around $\theta = (2n+1)\pi/4$, $n=0,\ldots,3$, where $R(\theta)$ is not defined. Therefore, one considers the analytical continuation $r(\theta)$ such that, in particular, $dr/d\theta = 0$ at $\theta = \pi/4$ as required by symmetry. This, together with continuity and analyticity, leads to a second order polynomial and its coefficients $r(\theta) = a\theta^2 + b\theta + c$.

Figure 7 illustrates the result. In equilibrium, $p=0$, the droplet tends to become squared as $T \to 0$ due to the underlying lattice anisotropy, while it recovers the (isotropic) spherical shape for $T \gtrsim 0.5T_O$. In nonequilibrium, the droplet adopts a shape which is intermediate between a circle and a square. This is again due to the fact that the temperature $T_{ef}^{(I)}$ that the interface *feels* does not go to zero as $T \to 0$ for any $p > 0$.

A more quantitative description is provided by the droplet form factor $\Omega_d(T,p)$. This is defined via the equality $V = \Omega_d(T,p)\mathcal{R}^d$, where $\mathcal{R} \equiv R(\theta=0)$ is a measure of the droplet radius and V is the droplet volume. For a two-dimensional system

$$\Omega(T,p) = 4\int_0^{\pi/4} d\theta \left(\frac{R(\theta)}{R(0)}\right)^2. \tag{18}$$

The square and circular droplets are characterized by $\Omega = 4$ and π, respectively. Figure 8 shows $\Omega(T,p)$ as a function of T for different values of p. This clearly demonstrates that $\Omega(T,p)$ goes to 4 (squared shape) in the low-T limit for $p=0$, but the tendency is towards a smaller value for any $p > 0$. That is, unlike in equilibrium at low enough temperature, no facets are expected in a nonequilibrium droplet.

V. CONCLUSIONS

This paper deals with the influence of a simple nonequilibrium condition, which may ideally represent the situation in a class of disordered systems,[10] on the microscopic and macroscopic properties of a complex interface. It is assumed that the probability of an discrete change by δ at the (nonequilibrium) interface is proportional to $X^{|\delta|}$, where $X = X(T,p)$ is the statistical weight of an interfacial broken bond for temperature T and nonequilibrium perturbation p.

This is expressed $X=\Sigma_\eta \Pi_\eta X_\eta$ in terms of the probability Π_η that an interfacial broken bond ends at a spin surrounded by certain degree η of local order.

Our main hypothesis consists in assuming that the nonequilibrium system is attempting to minimize a surface and, consequently, one may translate here the equilibrium formalism. It is also assumed that, at least for the model studied in this paper, the specific nonequilibrium mechanism simply adds to the basic thermal mechanism in such a way that it may be incorporated in a nonperturbative manner to the microscopic parameter $X(T,p)$. Therefore, this contains *all* the information concerning the effect of the nonequilibrium perturbation p on the interface, and it follows that a SOS theory based on $X(T,p)$ yields the microscopic and macroscopic behavior of the nonequilibrium interface. In this way, one may finally obtain an explicit expression for the relevant nonequilibrium surface tension $\sigma_{\rm NE}(T,p)$.

Regarding the microscopic interface structure, the nonequilibrium *noise* turns out to enhance interfacial fluctuations. In particular, the typical scale for interfacial fluctuations increases with p. It is also demonstrated that the nonequilibrium interface remains rough in the zero-T limit, contrary to the equilibrium case. These are theoretical predictions in full agreement with Monte Carlo simulations.

Regarding macroscopic behavior, $\sigma_{\rm NE}(T,p)$ exhibits *anomalous* behavior at low T (for any $p>0$). In particular, $\sigma_{\rm NE}$ is a nonmonotonous function of T with a maximum at $T=T_{\rm max}(p)$, and $\sigma_{\rm NE}$ decreases as the system is cooled further below $T_{\rm max}(p)$. This counterintuitive prediction is also confirmed indirectly by Monte Carlo simulations. That is, we estimated numerically the critical droplet size $R_c(T,p)$, which is expected to be proportional to the surface tension,[12] as the system exits from a metastable state. Some intuition on the origin of this anomaly is obtained by defining an interface effective temperature which importantly deviates from T. In this way, the nonmonotonous T dependence of $\sigma_{\rm NE}$ can be related to a crossover between two different temperature regimes: a low-T region dominated by the nonequilibrium noise, where $\sigma_{\rm NE}\propto T$, and a high-T regime dominated by thermal fluctuations, where $\sigma_{\rm NE}\propto\sigma_e$. The shape of the nonequilibrium droplet as obtained by a Wulff construction also reflects the anomaly of $\sigma_{\rm NE}$. We find, in particular, that droplets at very low temperature tend to minimize more their surface under the nonequilibrium condition.

These details are essential to nucleation theory. Therefore, we expect that the anomalous low-temperature behavior of the nonequilibrium surface tension described above may be relevant to many physical processes such as the ones mentioned in Sec. I. The possible utility of our results here will be addressed in a forthcoming paper concerning the relaxation of a nonequilibrium system from a metastable state.[12]

Finally, the results in this paper are explicitly obtained for a square lattice. Some caution should be used before generalizing, since there are examples when the shape and properties of a nonequilibrium interface depend strongly on the geometry of the host lattice.[29] However, we believe that the phenomenology here described should hold for more lattice geometries other than square, provided that the (nonequilibrium) interface endures an effective temperature with the same qualitative properties than the one discussed above, i.e., $T_{\rm ef}^{(I)}$ saturates to a constant p-dependent value as $T\to 0$ and is proportional to T at high enough temperature.

ACKNOWLEDGMENTS

We acknowledge very useful discussions with M.A. Muñoz, and financial support from MCYT-FEDER Project No. BFM2001-2841. P.I.H. also thanks the MECD for support.

[1] D. Jasnow, Rep. Prog. Phys. **47**, 1059 (1984).
[2] P.G. de Gennes, Rev. Mod. Phys. **57**, 827 (1985).
[3] D.E. Sullivan and M.M. Telo da Gama, *Fluid Interfacial Phenomena*, edited by C.A. Croxton, ed. (Wiley, New York, 1986).
[4] A.J. Bray, Adv. Phys. **43**, 357 (1994).
[5] A.-L. Barabási and H.E. Stanley, *Fractal Concepts in Surface Growth* (Cambridge University Press, Cambridge, 1995).
[6] A. Pimpinelli and J. Villain, *Physics of Crystal Growth* (Cambridge University Press, Cambridge, 1999).
[7] D. Bonn and D. Ross, Rep. Prog. Phys. **64**, 1085 (2001).
[8] A. Hernández-Machado, H. Guo, J.L. Mozos, and D. Jasnow, Phys. Rev. A **39**, 4783 (1989).
[9] B. Derrida, J.L. Lebowitz, E.R. Speer, and H. Spohn, Phys. Rev. Lett. **67**, 165 (1991).
[10] J. Marro and R. Dickman, *Nonequilibrium Phase Transitions in Lattice Models* (Cambridge University Press, Cambridge, 1999).
[11] P.I. Hurtado, Ph.D. thesis, Universidad de Granada, Granada, Spain, cond-mat/0302349.
[12] P.I. Hurtado, J. Marro, and P.L. Garrido (unpublished).
[13] P.I. Hurtado, J. Marro, and P.L. Garrido, Phys. Rev. E **70**, 021101 (2004).
[14] M. Kardar, G. Parisi, and Y.-C. Zhang, Phys. Rev. Lett. **56**, 889 (1986).
[15] J.E. Avron, H. van Beijeren, L.S. Schulman, and R.K.P. Zia, J. Phys. A **15**, L81 (1982).
[16] W.K. Burton, N. Cabrera, and F.C. Frank, Proc. R. Soc. London, Ser. A **243**, 299 (1951).
[17] S. Miracle-Sole and J. Ruiz, in *Micro, Meso and Macroscopic Approaches in Physics*, edited by A. Verbeure (Plenum, New York, 1993).
[18] P.A. Rikvold and M. Kolesik, J. Stat. Phys. **100**, 377 (2000).
[19] R.A. Blythe and M.R. Evans, Phys. Rev. Lett. **89**, 080601 (2002).
[20] H.N.V. Temperley, Proc. Cambridge Philos. Soc. **48**, 683 (1952).
[21] The frozen spins at the top and bottom rows are not taken into account when defining these classes. Since those spins do not change with time, they are considered to be *outside* the system, just inducing appropriate boundaries conditions. Notice, on the other hand, that an external magnetic field breaks the up-down symmetry, and ten different spin classes then emerge.

[22] For $\Psi(\Gamma)=e^{-\Gamma}(1+e^{-\Gamma})^{-1}$, all the functions $X_\eta(T,p)$ differ from each other, which makes the expressions and discussion concerning this point much more involved. However, the numerical differences between the two rates are negligible for all practical purposes here, so that we found it convenient to explicitly illustrate in this section the case $\Psi(\Gamma)=\min[1,e^{-\Gamma}]$ only.

[23] The SOS approximation would imply that $P(\delta,\epsilon)=XP(\delta)P(\epsilon)$ with $P(\delta)$ given in Eq. (3). One may then estimate $\Pi_\eta(T,p)$ as a function of $X(T,p)$, and a trascendental equation for $X(T,p)$ ensues which cannot be solved analytically. The higher order approximation that we present here provides an explicit expression.

[24] E. Müller-Hartmann and J. Zittartz, Z. Phys. B **27**, 261 (1977).

[25] C. van den Broeck, J.M.R. Parrondo, and R. Toral, Phys. Rev. Lett. **73**, 3395 (1994); Phys. Rev. E **55**, 4084 (1997); J.J. Torres, P.L. Garrido, and J. Marro, Phys. Rev. B **58**, 11 488 (1998); W. Genovese, M.A. Muñoz, and P.L. Garrido, Phys. Rev. E **58**, 6828 (1998); S. Mangioni, R. Deza, R. Toral, and H. Wio, *ibid.* **61**, 223 (2000); M. Ibañes, J. Garcia-Ojalvo, R. Toral, and J.M. Sancho, Phys. Rev. Lett. **87**, 020601 (2001).

[26] C. Rottman and M. Wortis, Phys. Rev. B **24**, 6274 (1981).

[27] G. Wulff, Z. Kristallogr. Mineral. **34**, 448 (1901); C. Herring, Phys. Rev. **82**, 87 (1951); in *Structure and Properties of Solid Surfaces*, edited by R. Gomer and C.S. Smith (University of Chicago Press, Chicago, 1953), pp. 5–72.

[28] See Appendix D in Ref. 16.

[29] S.C. Glotzer, D. Stauffer, and N. Jan, Phys. Rev. Lett. **72**, 4109 (1994); S. Toxvaerd, Phys. Rev. E **53**, 3710 (1996); A. Szolnoki, *ibid.* **60**, 2425 (1999); F.J. Alexander, C.A. Laberge, J.L. Lebowitz, and R.K.P. Zia, J. Stat. Phys. **82**, 1133 (1996).